Adaptive Predictive Power Control for the Uplink Channel in DS-CDMA Cellular Systems

Mansour A. Aldajani, *Member, IEEE*, and Ali H. Sayed, *Fellow, IEEE*

Abstract—In this paper, we analyze the conventional closed-loop power-control system. We explain that the system behaves essentially as a companded delta modulator and then derive an expression for the power-control error in terms of the channel fading, which suggests methods for reducing the error variance. This is achieved by using a prediction technique for estimating the channel-power fading profile. The prediction module is combined with several proposed schemes for closed-loop power control. The resulting architectures are shown to result in improved performance in simulations.

Index Terms—Adaptive filtering, channel inverse coding, closed loop, direct sequence code division multiple access (DS-CDMA), error analysis, power control, prediction, Rayleigh fading.

I. INTRODUCTION

THE requirement of power control (PC) in the uplink direct-sequence code-division multiple-access (DS-CDMA) system is a critical limitation [1]. Power control is needed because all users share the same bandwidth and, thus, interuser interference is bound to occur. Without power control, a signal received by the base station (BS) from a nearby mobile station (MS) will dominate the signal from a far-away MS, resulting in the so-called *near–far effect*. The objective of power control is to control the transmitted power by the mobile units so that the average power received from each unit is generally constant. Some of the main advantages of power control can be summarized as follows.

1) Power control reduces interuser interference by overcoming the near–far effect, which results in capacity increase of the overall CDMA system.
2) Power control combats the Rayleigh-fading channel effect on the transmitted signal by compensating for the fast fading of the wireless channel. This reduces the required signal-to-noise ratio (SNR) E_b/N_o. In perfect power-control conditions, power control turns a fading channel into an additive white Gaussian noise (AWGN) [1].
3) Power control minimizes the power consumption of the mobile units. Instead of using a fixed maximum power by the MS, it will now use an adaptive transmission power based on the power-control requirements.

In closed-loop power control (CLPC), the BS measures the fading effects in the signal received from each mobile station by measuring the signal power and the bit-error rate (BER). Typically, the received power is measured by averaging multiple samples of the received sequence, while the BER is computed by comparing the received sequence with a predetermined transmitted sequence. The BS then compares these quantities with a reference point. Based on this comparison, the BS transmits a one-bit signal, known as the *power bit*, to each MS, commanding it to either increase or decrease its power by a fixed amount, e.g., 1, 0.5, or 0.25 dB. The power bit rate is 800 Hz in IS-95 standards and 1500 Hz in 3G WCDMA standards. Fig. 1 shows a block-diagram representation of the conventional CLPC scheme. In the downlink channel, power control is not required since all signals to the different MS are initiated from the same source.

A. Limitations of Conventional CLPC

The performance of conventional CLPC is limited for at least two reasons. First, the delta modulator-like behavior of the conventional CLPC is slow in tracking fast and deep fading of the wireless channel. This effect creates what is known in the delta-modulation context as *slope overload*. In addition, the CLPC creates a noisy response known as *granular noise* when the fading is smooth or minimal. In the literature, there are two main methods that have been used to improve the performance of the conventional CLPC, namely adaptive step size and predictive power control.

In adaptive step-size power control, the step size of the power-error quantizer is adapted in a way to cope with quickly changing channel-fading effects. Examples of such schemes can be found in [2]–[6]. Predictive power control, on the other hand, is based on predicting the channel attenuation one step ahead [7]–[9]. The predicted value is then used in calculating the predicted received power.

In this paper, we start from the power-control loop of Fig. 1. We derive a closed-form expression for the power error in terms of the channel fading and the desired power, and use this expression to evaluate the mean and variance of the power-error signal. We then propose four algorithms that attempt to minimize the error variance. These algorithms require the prediction of the channel fading (a prediction scheme is developed for this purpose). Simulations of the proposed algorithms show an improved power-control performance over conventional CLPC.

For the sake of simplicity, two assumptions are made in this paper. First, it is assumed that the received power is estimated with no errors (i.e., the estimated power equals the received
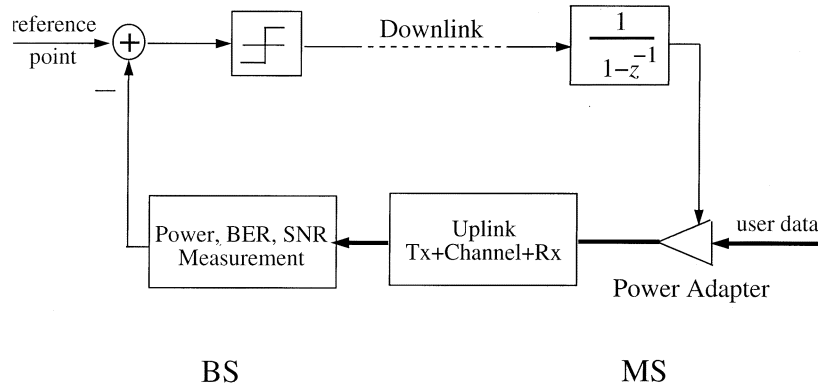
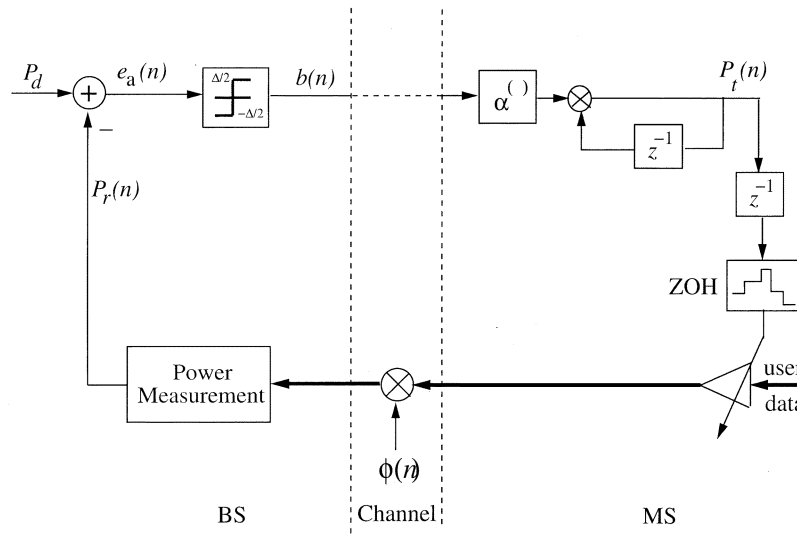Fig. 1.   Conventional closed-loop power control.

Fig. 2.   Conventional CLPC.

power). Second, the power-control feedback loop is assumed to be error-free (the BER of the power bit is zero).

II. ANALYSIS OF CONVENTIONAL CLPC

A. Power-Channel Model

We assume a multipath channel with Rayleigh-fading reflections that are optimally combined using a RAKE receiver with M fingers. The discrete-time received power $P_r(n)$ at the BS can be expressed as [9], [10]

$$P_r(n) = \frac{1}{T_p} \int_{(n-1)T_p}^{nT_p} P_t(t)Q(t)dt \qquad (1)$$

where T_p is the power-control period, $P_t(t)$ is the transmitted power, and $Q(t)$ is the power gain of the channel. This gain contains all effects of the multipath reflections on the signal power. In [10], the gain $Q(t)$ is given by

$$Q(t) = \sum_{p=0}^{L-1} |a_p(t)|^2 \qquad (2)$$

where $a_p(t)$ is the tap weight coefficient relative to the pth finger of the RAKE receiver. The transmission power $P_t(t)$ is kept unchanged during a power-control period so that

$$P_r(n) = P_t(n-1) \left[\frac{1}{T_p} \int_{(n-1)T_p}^{nT_p} Q(t)dt \right]. \qquad (3)$$

If we define

$$\phi(n) \triangleq \frac{1}{T_p} \int_{(n-1)T_p}^{nT_p} Q(t)dt \qquad (4)$$

then the received power is given by

$$\boxed{P_r(n) = \phi(n)P_t(n-1).} \qquad (5)$$

B. Equivalent Model for Conventional CLPC

Fig. 2 shows a more-detailed block diagram of the conventional CLPC. The transmission power $P_t(t)$ used by the MS is attenuated by the channel fading $\phi(n)$. At the BS, the received power $P_r(n)$ is measured. (We assume an exact power measurement.) The received power $P_r(n)$ is then compared to a desired fixed power level P_d. The error $e_a(n)$ is defined by

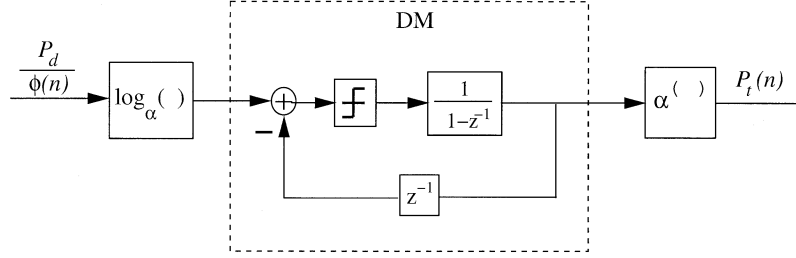$$e_a(n) = P_d - P_r(n). \qquad (6)$$

Fig. 3. Equivalent structure for conventional CLPC.

Equivalently, using (5), we can write

$$e_a(n) = P_d - \phi(n)P_t(n-1). \qquad (7)$$

The power error $e_a(n)$ is quantized using a one-bit quantizer to produce the power-command bit (PCB) $b(n)$, scaled by half the step size of the quantizer Δ, i.e.,[1]

$$b(n) = \frac{\Delta}{2}\text{sign}[e_a(n)]. \qquad (8)$$

This PCB is transmitted to the MS, which then increments or decrements its transmission power by a fixed amount (in decibels), say

$$P_t(n) = \alpha^{b(n)}P_t(n-1) \qquad (9)$$

where α is a constant (usually $1 < \alpha < 3$). In other words, $P_t(n)$ is incremented or decremented by ψ dB where

$$\psi = 10\log_{10}\alpha. \qquad (10)$$

If we take the logarithm of both sides of (9)

$$\log_\alpha P_t(n) = b(n) + \log_\alpha P_t(n-1) \qquad (11)$$

and use (7) and (8), we get

$$b(n) = \frac{\Delta}{2}\text{sign}[P_d - \phi(n)P_t(n-1)]. \qquad (12)$$

Now, since the logarithm is an increasing function, we can rewrite this equation as

$$b(n) = \frac{\Delta}{2}\text{sign}[\log_\alpha P_d - \log_\alpha(\phi(n)P_t(n-1))]. \qquad (13)$$

Equivalently

$$b(n) = \frac{\Delta}{2}\text{sign}[\log_\alpha P_d - \log_\alpha \phi(n) - \log_\alpha P_t(n-1)]. \qquad (14)$$

Therefore

$$b(n) = \frac{\Delta}{2}\text{sign}\left[\log_\alpha\left(\frac{P_d}{\phi(n)}\right) - \log_\alpha P_t(n-1)\right]. \qquad (15)$$

Substituting this expression into (11), we get

$$\log_\alpha P_t(n) = \log_\alpha P_t(n-1) + \frac{\Delta}{2}\text{sign}[\log_\alpha\left(\frac{P_d}{\phi(n)}\right)\log_\alpha P_t(n-1)]. \qquad (16)$$

This expression shows that, in the logarithmic scale, the relation between $\{P_d, P_t(n)\}$ amounts to a delta-modulation (DM) scheme with input $\log_\alpha(P_d/\phi(n))$ and output $\log_\alpha P_t(n)$, as shown in Fig. 3. The logarithm function is added before the

[1]We shall assume that the error signal $e_a(n)$ is small enough so that the single-bit quantizer of Fig. 2 behaves like the signum function in (8).

DM, while an exponential function is added after the DM to get $P_t(n)$.

In other words, the result (16) shows that the conventional CLPC model of Fig. 2 is actually a companded delta modulator with input $P_d/\phi(n)$ and output $P_t(n)$. In this way, the CLPC attempts to make the transmission power $P_t(n)$ track the quantity $P_d/\phi(n)$ using a companded delta modulator. The results obtained in this section essentially match the *log-linear* model used in [10] and [11]. Now, we continue with a linear analysis model by following the method of [12] on companded DM systems.

C. Power-Control Error

DM is a simple tracking mechanism that is used in coding and data conversion. Fig. 4(a) shows a block diagram of a DM. A linearized version of DM can be obtained by modeling the effect of the quantizer as an additive quantization noise $e_d(n)$, as shown in Fig. 4(a).

The quantization error $e_d(n)$ is usually assumed to be uniformly distributed between $[-\Delta/2, \Delta/2]$, where Δ is the step size of the quantizer. The transfer function of the linearized DM is then given by

$$Y_d(z) = X_d(z) + E_d(z). \qquad (17)$$

In the time domain

$$y_d(n) = x_d(n) + e_d(n). \qquad (18)$$

Referring to Fig. 3 and using the linearization of Fig. 4 for the DM, we can argue by following the derivation in [12] that the relation of $P_t(n)$ to $\log_\alpha(P_d/\phi(n))$ can be approximated via a random gain model as

$$P_t(n) = \alpha^{\log_\alpha(P_d/\phi(n))}K(n) = \frac{P_d}{\phi(n)}K(n) \qquad (19)$$

where $K(n)$ is a random variable that is defined by

$$K(n) = \alpha^{e_d(n)}. \qquad (20)$$

If we substitute (19) into (5), we find that

$$\boxed{P_r(n) = \frac{\phi(n)}{\phi(n-1)}P_d(n-1)K(n-1).} \qquad (21)$$

For the sake of compactness, let us introduce the notation

$$\boxed{\overline{(\cdot)} \triangleq 10\log_{10}(\cdot)} \qquad (22)$$

and use it to write (21) as

$$\overline{P}_r(n) = \overline{\phi}(n) - \overline{\phi}(n-1) + \overline{P}_d + \overline{K}(n-1). \qquad (23)$$
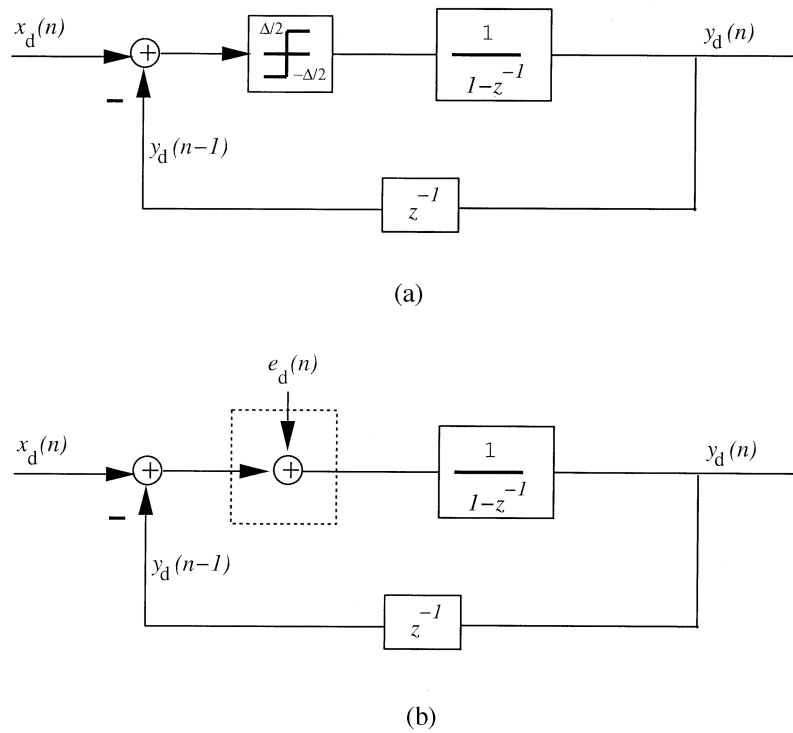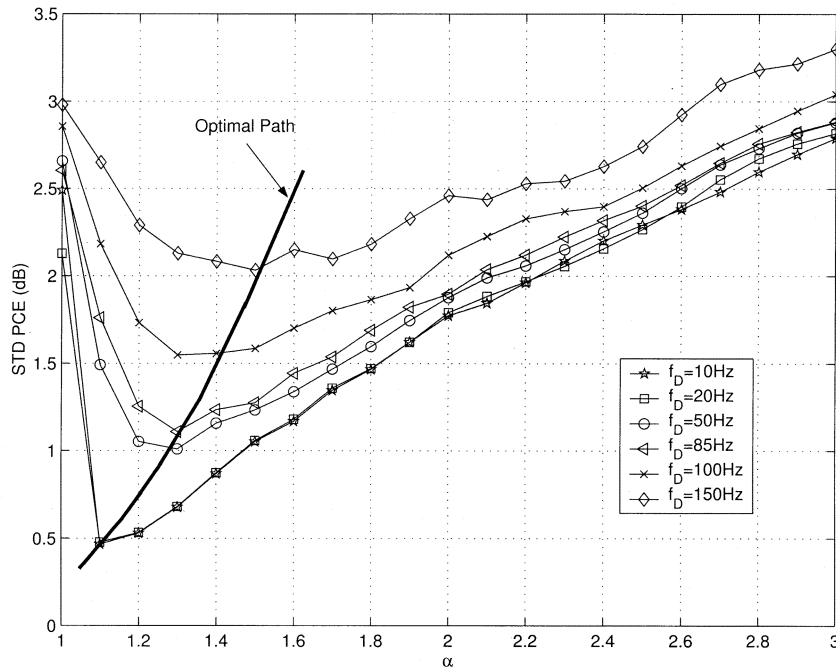
(a)

(b)

Fig. 4.   A linearized DM.

Fig. 5.   Performance of conventional CLPC versus α for different Doppler frequencies.

But since $K(n) = \alpha^{e_d(n)}$ and $\overline{\alpha} = 10 \log_{10} \alpha = \psi$, then

$$\overline{K}(n) = \psi e_d(n). \qquad (24)$$

Substituting (24) into (23), we arrive at the following expression for the received power in the logarithmic scale:

$$\boxed{\overline{P}_r(n) = \overline{\phi}(n) - \overline{\phi}(n-1) + \overline{P}_d + \psi e_d(n-1).} \qquad (25)$$

Let us define the closed-loop power-control error (PCE) in decibels as[2]

$$e(n) \triangleq \overline{P}_r(n) - \overline{P}_d = 10 \log_{10} \left(\frac{P_r(n)}{P_d} \right). \qquad (26)$$

[2]This error is just another way of measuring the difference between $P_r(n)$ and P_d. It employs a logarithmic scale, while the earlier error, $e_a(n)$, defined in Fig. 2, employs a linear scale.
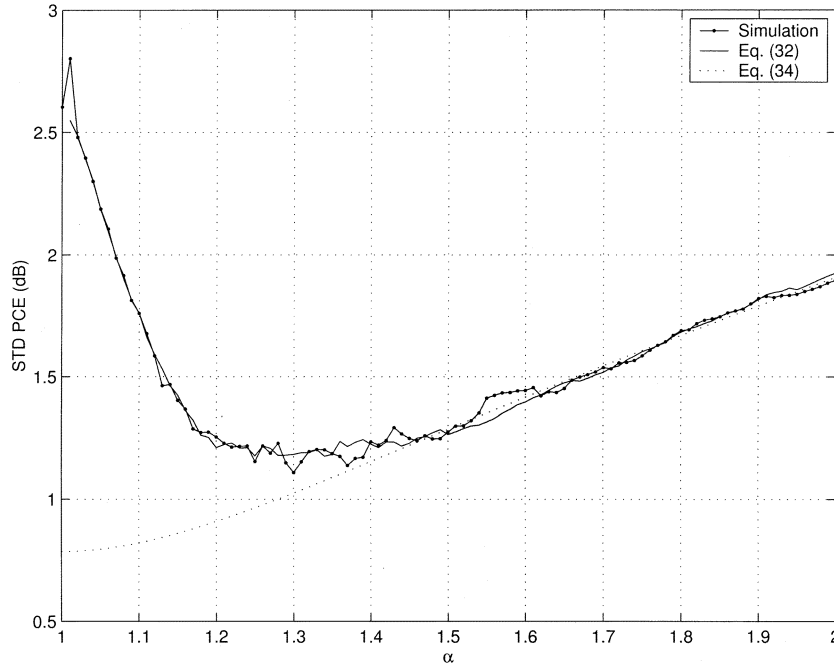
Fig. 6.   Comparison between the power-error-variance expressions (32) and (34) with simulation results.

Then, from (25)

$$e(n) = \overline{\phi}(n) - \overline{\phi}(n-1) + \psi e_d(n-1). \tag{27}$$

This expression shows that the power error $e(n)$ is affected by the following two factors:

1) variation in the channel-power fading $\overline{\phi}(n) - \overline{\phi}(n-1)$.
2) quantization noise $e_d(n)$.

In Sections II-D and II-E, we derive expressions for the mean and variance of $e(n)$. To do so, we will make the following assumptions.

A.1) $e_d(n)$ is a uniformly distributed random variable within $[-\Delta/2, \Delta/2]$. This is reasonable under the approximation that $e_a(n)$ of Fig. 2 lies within $[-\Delta/2, \Delta/2]$.
A.2: All random processes are stationary and independent of each other.

D. Mean and Variance Analysis

Taking the expected value of both sides of (27), we have

$$E\{e(n)\} = E\left\{\overline{\phi}(n)\right\} - E\left\{\overline{\phi}(n-1)\right\} + \psi E\{e_d(n-1)\}. \tag{28}$$

However, since by stationarity and at steady state

$$E\{\overline{\phi}(n)\} = E\{\overline{\phi}(n-1)\} \triangleq E_{\overline{\phi}}$$

and since $E\{e_d(n-1)\} = 0$, we conclude that

$$E_e \triangleq E\{e(n)\} = 0. \tag{29}$$

To evaluate the variance of $e(n)$, we square both sides of (27) to get

$$e^2(n) = \left(\overline{\phi}(n) - \overline{\phi}(n-1)\right)^2 \\ + 2\left(\overline{\phi}(n) - \overline{\phi}(n-1)\right)\psi e_d(n-1) \\ + \psi^2 e_d^2(n-1). \tag{30}$$

Using the uncorrelatedness assumption A.1

$$E\left\{\left(\overline{\phi}(n) - \overline{\phi}(n-1)\right)\psi e_d(n-1)\right\} = 0 \tag{31}$$

we find that

$$E\{e^2(n)\} = E\{\left(\overline{\phi}(n) - \overline{\phi}(n-1)\right)^2\} \\ + \psi^2 E\left\{e_d^2(n-1)\right\}. \tag{32}$$

When the uniformity assumption A.2 on the quantization noise $e_d(n)$ is reasonable, we further have

$$E\{e_d^2(n-1)\} = \int_{-(\Delta/2)}^{\Delta/2} \frac{1}{\Delta} x^2 dx = \frac{\Delta^2}{12} \tag{33}$$

so that the power error variance can be expressed as

$$E\{e^2(n)\} = E\{\left(\overline{\phi}(n) - \overline{\phi}(n-1)\right)^2\} + \psi^2 \frac{\Delta^2}{12}. \tag{34}$$

Expression (32) is more general in that it does not rely on the uniformity assumption on $e_d(n)$. We summarize the result in the following statement.

1) Lemma: Power Control Error (PCE): For the CLPC scheme of Fig. 2, the PCE $e(n) \equiv \overline{P}_r(n) - \overline{P}_d$ is zero mean and its variance is given by (32). When the uniformity assumption on the quantization noise is reasonable, the error variance is given by (34).   ◇

E. Effect of the Choice of α

Referring to the companded DM structure of Fig. 3, we see that there are some restrictions on the choice of the positive quantity α. Clearly, α cannot be less than unity since it will then expand (rather than compress) the input to the DM. This will result in slope overload, in which case the DM will not be able to cope with the large variations in the input. Furthermore, α cannot be unity since this choice makes the system functionless ($P_t(n) = P_t(n-1)$). The larger than 1 the value of α is, the less slope overload there is in the system (i.e., the easier the tracking for the DM will be). However, from (27), increasing α
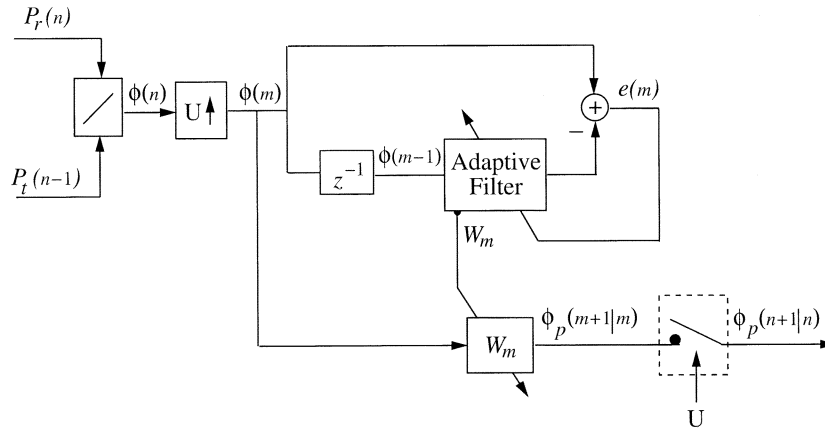
Fig. 7. Power-fading prediction.

will increase the power-tracking error, thus putting a limitation on how large α can be.

To examine the effect of α on the PCE, we choose a certain Doppler frequency[3] f_D and generate the corresponding power-fading signal $\phi(n)$. We also choose a value for the exponent term α and run a simulation implementing the CLPC of Fig. 2. The standard deviation (STD) of the error signal $e(n)$ is measured. The values of f_D and α are then changed and the STD is measured again. The result is shown in Fig. 5, which shows that the optimal choice of α lies within the interval [1], [2]. The heavy solid curve indicates the optimal path of α as a function of f_D.

Fig. 6 shows a comparison between the simulation and analytical results of the PCE standard deviation with $f_D = 85$ Hz. The figure shows two curves associated with (32) and (34).

The theoretical curve from (32) shows a strong match with the simulation results for $1 < \alpha < 2$. On the other hand, the theoretical curve associated with (34) matches the simulation results only for large enough α. Recall that (32) assumes that the second moment of the quantization error $e_d(n)$ can be estimated. On the other hand, (34) relies on the uniformity assumption for the quantization error (which is dependent upon α and the amount of slope overload in the DM). These observations support our conclusion that (34) should be used only if the uniformity assumption on $e_d(n)$ is reasonable. Otherwise, (32) gives a more-accurate characterization of system performance.

III. OVERSAMPLED CHANNEL PREDICTION

The CLPC methods that we will propose in the sequel will require a prediction for the channel power fading profile $\phi(n)$. In this section, we propose one method for predicting $\phi(n)$, which is based on oversampling the received power variations at the BS. Then, a normalized least mean squares (NLMS)-based adaptive predictor is used to estimate the channel fading one step ahead. To do so, we assume that the BS knows the transmitted power $P_t(n)$ of the MS at each time instant. This assumption is reasonable in CLPC since the BS can usually recover $P_t(n)$ from the information sent to the MS.

[3]The Doppler frequency f_D is the width of the Doppler power spectrum of the wireless channel. The Doppler frequency and the delay spread of the channel are reciprocally related [13].

Fig. 7 shows the structure of the proposed prediction method. The measured received power $P_r(n)$ is divided by $P_t(n-1)$ to get the power attenuation $\phi(n)$, i.e.,

$$\phi(n) = \frac{P_r(n)}{P_t(n-1)}. \tag{35}$$

The signal $\phi(n)$ is then up-sampled by a factor of U, resulting in $\phi(m)$, where m refers to the oversampling index. This can be achieved by increasing the sampling rate of the received power and by assuming that the transmission power is constant between two consecutive samples of $P_t(n)$.

The signal $\phi(m)$ is then passed through a delay, as shown in Fig. 7. The delayed samples $\phi(m-1)$ are fed into an adaptive filter of order M. The output of the adaptive filter is compared to $\phi(m)$ and the comparison error is fed back to the adaptive filter for training. The taps of the adaptive filter W_m extract the correlation between the fading samples. The tap values are carried out and used to adapt the taps of an finite-impulse-response (FIR) filter, as shown in the figure. The input to this FIR filter is $\phi(m)$ and its output is the prediction of $\phi(m+1)$, denoted by $\phi_p(m+1|m)$. This signal is then down-sampled by the same factor U to produce the required prediction value

$$\phi_p(n+1|n) \approx \phi(n+1). \tag{36}$$

The normalized LMS algorithm [14] is used whereby the $(M \times 1)$ tap vector W_m is updated according to the rule

$$W_{m+1} = W_m + \frac{\mu}{\delta + \|\mathbf{u}_m\|^2} \mathbf{u}_m^* [\phi(m) - \mathbf{u}_m W_m] \tag{37}$$

where the regression vector $\mathbf{u}_m$ contains the prior M samples of $\phi(m-1)$ and the notation $\|\cdot\|^2$ denotes the Euclidean norm. The constant μ is the step size of the adaptive filter and δ is an arbitrary small positive number.

The performance of this predictor is dependent upon many factors, such as the filter type, order, and step size. Furthermore, the oversampling factor U plays a useful role in the performance of the predictor, since it helps increase the correlation between the samples of $\phi(m)$. It should be noted that increasing U will also introduce noise in the measured $P_r(n)$, resulting in a degradation in performance. This usually sets an upper limit for the choice of U. Through simulations, we found that $U \leq 5$ is an acceptable choice. Fig. 8 shows an attenuation curve $\phi(n)$ resulting from a
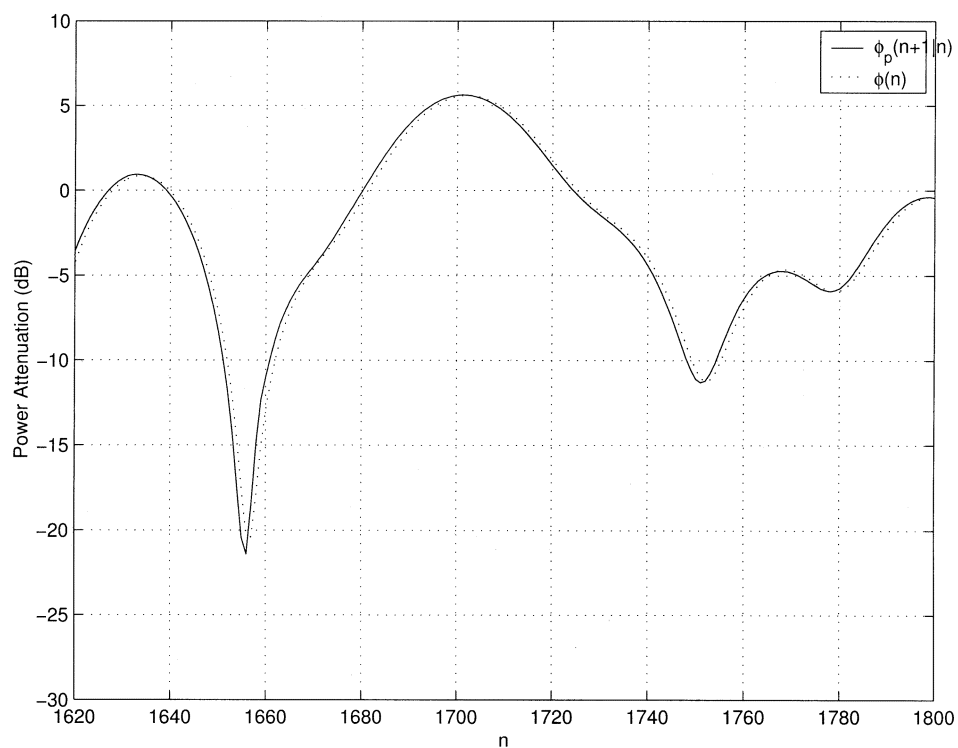
Fig. 8. Time response of the channel attenuation and its prediction for a Rayleigh-fading channel.
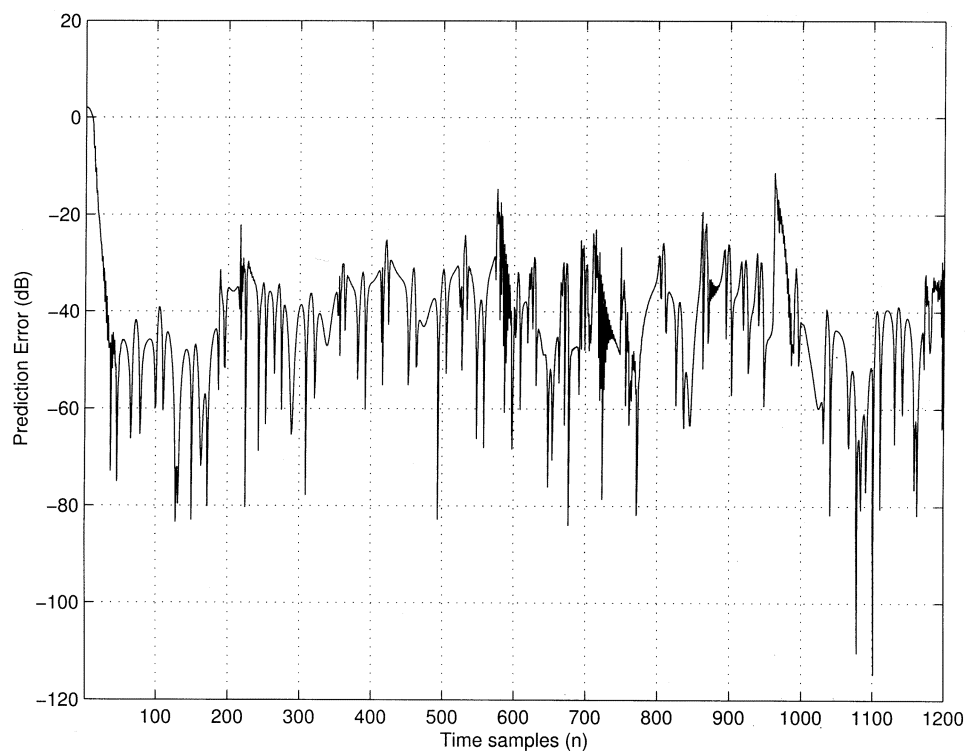

Fig. 9. Prediction error over time for a Rayleigh-fading channel with $f_D = 50$ Hz and $U = 1$.

Rayleigh-fading channel together with its predicted value $\phi_p(n + 1|n)$.

Fig. 9 shows a plot of the prediction error $e_{pr} = \phi_p(n + 1|n) - \phi(n + 1)$ over time for a Rayleigh-fading channel with $f_D = 50$ Hz, $U = 1$, and $\mu = 1.8$. The error decays to -40 dB and stays under -30 dB for most of the simulation time. In Fig. 10, we show the prediction mean square error (MSE) $E\{e_{pr}^2\}$ versus the step size μ for different Doppler frequen-
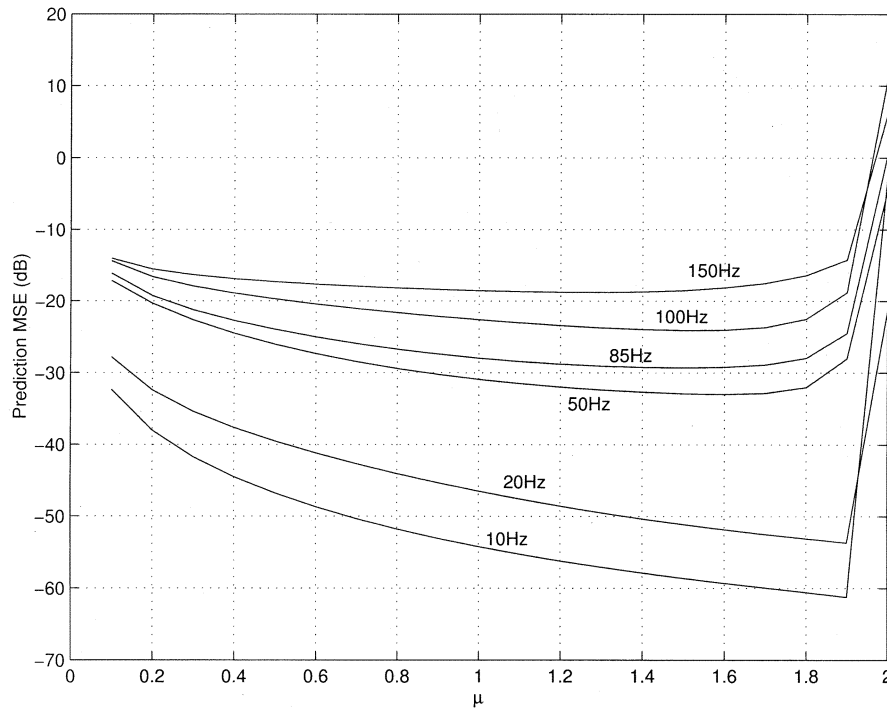
Fig. 10.   Effect of the step size μ on prediction MSE for different Doppler frequencies.
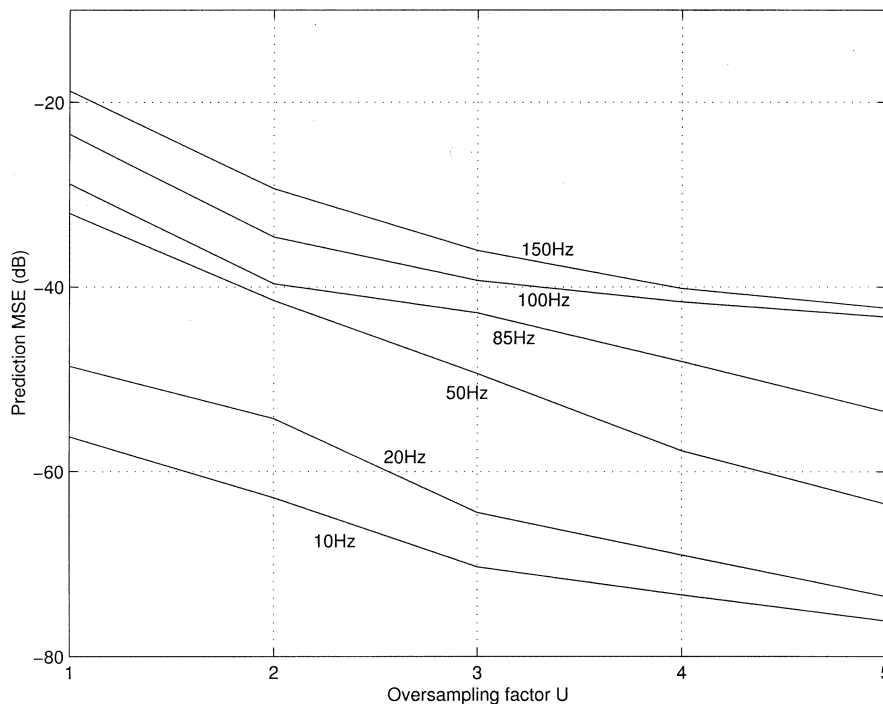

Fig. 11.   The prediction MSE as a function of the oversampling factor U for different Doppler frequencies.

cies. For high Doppler frequencies, the PCE is less affected by the choice of μ. Moreover, abrupt changes to the STD occur when μ is greater than 1.9. A reasonable choice for μ lies in the interval (1.6,1.8).

The MSE can be reduced by increasing the oversampling factor U. In Fig. 11, the MSE is shown as a function of U for different f_Ds and for $\mu = 1.2$. As is seen, increasing the over-sampling rate improves the prediction quality that, in turn, re-sults in better tracking performance. In practice, there is a limit on how large U can be. As we mentioned earlier, increasing U decreases the averaging period of the measured power, which may increase the power-measurement error.
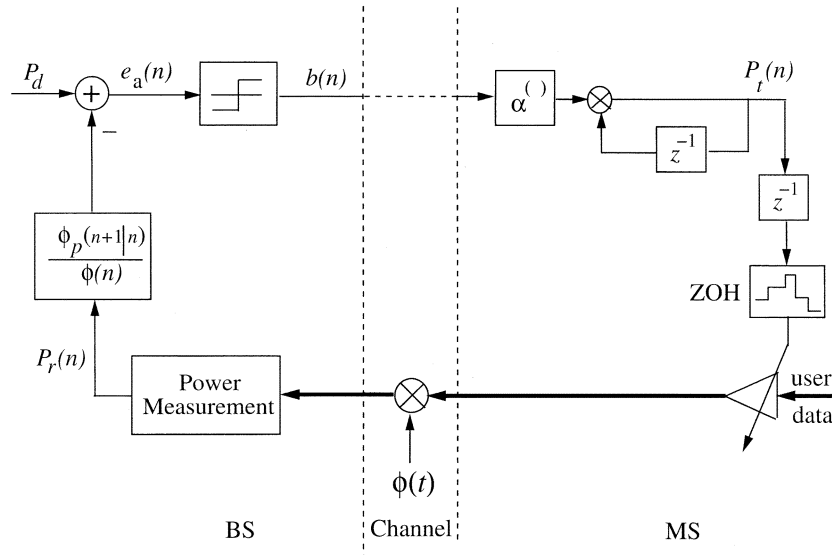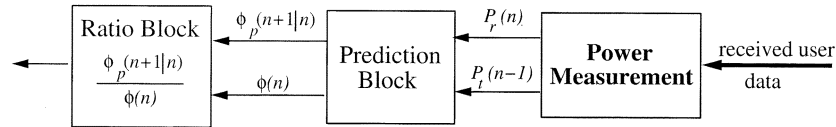
Fig. 12.   Block diagram of predictive ratio CLPC.

Fig. 13.   Evaluation of the predictive ratio. The prediction scheme used here is the one of Fig. 7.

IV. ALGORITHMS FOR ADAPTIVE CLPC

We now propose several algorithms for CLPC. The first is based on minimizing the difference $[\overline{\phi}(n) - \overline{\phi}(n-1)]$ that appears in (27) by replacing $\overline{\phi}(n-1)$ with its one-step prediction. The second algorithm is similar to the first, except that the exponent term α is adapted. In the third algorithm, the BS directly computes the prediction of the power attenuation caused by the channel. This information is sent to the MS after being source coded to meet the power bit-rate requirements. The MS will then use this information directly as its transmission power. The fourth algorithm is similar to the previous one, except that a more-powerful coding scheme is used. In Sections IV-A–D, we describe these algorithms in some detail. The prediction method described in the previous section is used by all four algorithms.

A. Algorithm 1: Predictive-Ratio CLPC (PR-CLPC)

The block diagram of this first scheme is shown in Fig. 12. The only modification relative to the conventional CLPC of Fig. 2 is the introduction of the ratio block $(\phi_p(n+1|n)/\phi(n))$. This will cancel the fading $\phi(n)$ caused by the channel and replace it with the prediction $\phi_p(n+1|n)$. Everything else is the same as in the conventional CLPC of Fig. 2.

If we follow the same derivation as in Sections II-B and C, we can verify that

$$P_t(n) = \frac{P_d}{\phi_p(n+1|n)} K(n) \qquad (38)$$

so that the received power is now given by

$$P_r(n) = \phi(n) P_t(n-1)$$
$$= \frac{\phi(n)}{\phi_p(n|n-1)} P_d(n-1) K(n-1).$$

If we take the logarithm of both sides, as we did in Section II-C, we get

$$\overline{P}_r(n) = \overline{\phi}(n) - \overline{\phi}_p(n|n-1) + \overline{P}_d + \overline{K}(n-1). \qquad (39)$$

In other words

$$\overline{P}_r(n) = \overline{\phi}(n) - \overline{\phi}_p(n|n-1) + \overline{P}_d + \psi e_d(n-1) \qquad (40)$$

and, hence, the power error is now given by

$$e(n) = \overline{\phi}(n) - \overline{\phi}_p(n|n-1) + \psi e_d(n-1). \qquad (41)$$

Note that the only difference between the conventional error expression (27) and the new expression (41) is that the term $\overline{\phi}(n-1)$ is replaced by $\overline{\phi}_p(n|n-1)$. The power error is now dependent upon the difference $[\overline{\phi}(n) - \overline{\phi}_p(n|n-1)]$ rather than $[\overline{\phi}(n) - \overline{\phi}(n-1)]$, as in conventional CLPC. Since, for reasonable prediction, $\overline{\phi}_p(n|n-1)$ is usually closer to $\overline{\phi}(n)$ than $\overline{\phi}(n-1)$, we expect this algorithm to result in lower PCE. The prediction term $\overline{\phi}_p(n|n-1)$ can be evaluated by resorting to the scheme of Fig. 7. In this way, the power measurement and ratio blocks on the left-hand side of Fig. 12 (at the BS side) can be more explicitly detailed, as shown in Fig. 13.

TABLE I
SUMMARY OF THE PREDICTIVE-RATIO CLPC (PR-CLPC) ALGORITHM

Initialization:
Choose the desired received power P_d.
Choose α and evaluate ψ from (10).
Choose the prediction parameters:
    Filter order, μ, and U.

For every CLPC time sample $n > 0$ do:

BS.

1. Measure $P_r(n)$ from the received sequence.
2. Knowing $P_t(n-1)$, estimate $\phi(n)$.
3. Evaluate $\phi_p(n+1|n)$.
4. Multiply $P_r(n)$ by $\frac{\phi_p(n+1|n)}{\phi(n)}$.
5. Compare the result with P_d:
    if $P_r(n)\frac{\phi_p(n+1|n)}{\phi(n)} > P_d$ then $b(n) = 1$
    else $b(n) = -1$
    end.
6. Send $b(n)$ to the MS.

MS

7. Extract $b(n)$ from the received data.
8. If $b(n) = 1$: increment $P_t(n)$ by ψdB
    else: decrement $P_t(n)$ by ψdB
    end.

TABLE II
SUMMARY OF THE ADAPTIVE PREDICTIVE-RATIO
CLPC (APR-CLPC) ALGORITHM

Initialization:
Choose the desired received power P_d.
Choose the adaptation parameters:
    C, α_{max} and α_{min}.
Choose the prediction parameters:
    Filter order, μ, and U.

For every CLPC time sample $n > 0$ do:

BS.

1. Measure $P_r(n)$ from the received sequence.
2. Knowing $P_t(n-1)$, estimate $\phi(n)$.
3. Evaluate $\phi_p(n+1|n)$.
4. Multiply $P_r(n)$ by $\frac{\phi_p(n+1|n)}{\phi(n)}$.
5. Compare the result with P_d:
    if $P_r(n)\frac{\phi_p(n+1|n)}{\phi(n)} > P_d$ then $b(n) = 1$
    else $b(n) = -1$
    end.
6. Send $b(n)$ to the MS.

MS

7. Extract $b(n)$ from the received data.
8. From $b(n-i)$, $i = 0, 1, 2$, compute $\lambda(n)$.
9. From (45) and (48) compute $\alpha(n)$ and $\psi(n)$.
10. If $b(n) = 1$: increment $P_t(n)$ by $\psi(n)$dB
    else: decrement $P_t(n)$ by $\psi(n)$dB
    end.

We can evaluate the mean and variance of the power error by following the same procedure and assumptions as in the conventional case of Section II-C. The error mean is given by

$$E\{e(n)\} = E\{\overline{\phi}(n)\} - E\{\overline{\phi}_p(n|n-1)\}$$
$$+\psi E\{e_d(n-1)\} = 0 \quad (42)$$

and the error variance by

$$E\{e^2(n)\} = E\left\{\left(\overline{\phi}(n) - \overline{\phi}_p(n|n-1)\right)^2\right\}$$
$$+\psi^2 E\left\{e_d^2(n-1)\right\}. \quad (43)$$

Again, when the uniformity assumption on the quantization noise $e_d(n)$ is reasonable, we get

$$E\left\{e^2(n)\right\} = E\left\{\left(\overline{\phi}(n) - \overline{\phi}_p(n|n-1)\right)^2\right\} + \psi^2\frac{\Delta^2}{12}. \quad (44)$$

Therefore, the variance of the PCE is now dependent upon the second moment

$$E\left\{\left(\overline{\phi}(n) - \overline{\phi}_p(n|n-1)\right)^2\right\}$$

and not on $E\left\{\left(\overline{\phi}(n) - \overline{\phi}(n-1)\right)^2\right\}$, as in the conventional case. Thus, any prediction with acceptable accuracy will improve the PCE. The PR-CLPC algorithm is summarized in Table I.

B. Algorithm 2: Adaptive Predictive-Ratio CLPC (APR-CLPC)

Here, we use an adaptation technique to vary the exponent term α (which determines the value of ψ). The motivation behind this algorithm is the following. When the channel-fading variations are small, the predictor performs well. Therefore, we can decrease α in order to decrease the power error of (27). When the variations are large, α is increased to boost the tracking capabilities of the power-control loop. The adaptation scheme used for α is

$$\alpha(n) = \alpha(n-1) + \lambda(n)C \quad (45)$$

where C is a positive constant, usually $C < 1$ (e.g., $C = 0.2$). The signal $\lambda(n)$ is chosen as

$$\lambda(n) = \begin{cases} +1 & \text{if } b(n) = b(n-1) = b(n-2) \\ -1 & \text{if } b(n) \neq b(n-1) \\ 0 & \text{otherwise .} \end{cases} \quad (46)$$

Furthermore, the exponent term $\alpha(n)$ is limited by lower and upper bounds, i.e.,

$$\alpha(n) = \begin{cases} \alpha_{\max}, & \text{if } \alpha(n) > \alpha_{\max}, \\ \alpha_{\min} & \text{if } \alpha(n) < \alpha_{\min} \end{cases}. \quad (47)$$

The bounds $\alpha_{\max}$ and $\alpha_{\min}$ are chosen from within the interval $(1, 3]$ (e.g., $\alpha_{\max} = 2.5$ and $\alpha_{\min} = 1.1$). The step change of $P_t(n)$ in decibels is

$$\psi(n) = 10\log_{10}\alpha(n). \quad (48)$$

The APR-CLPC algorithm is summarized in Table II.

C. Algorithm 3: Direct-Inverse CLPC (DI-CLPC)

Algorithms 1 and 2 attempt to minimize the power-error expression (27). In the third algorithm, we implement a direct inverse approach in which the MS is asked to transmit power in proportion to the inverse of the channel fading. A previously developed coder will be used to code the power information. This one-bit coder features high dynamic range and SNR performance, making it suitable for this application.

A block diagram of the scheme is shown in Fig. 14. The power-control process works as follows. The BS measures the received power $P_r(n)$ from the bit stream arriving at its end. Then, the MS transmission power $P_t(n-1)$ and $P_r(n)$ are fed to the prediction block, which produces $\phi_p(n+1|n)$, as in Fig. 13. The BS estimates the transmission power that should be used by the MS as

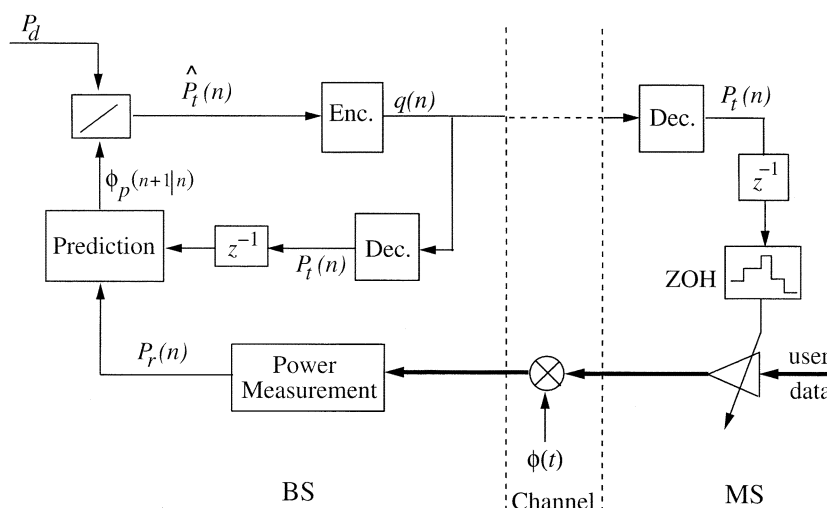$$\widehat{P}_t(n) = \frac{P_d}{\phi_p(n+1|n)}. \quad (49)$$

Fig. 14. Block diagram of the direct inverse CLPC algorithm. The prediction scheme of Fig. 7 can be used here.
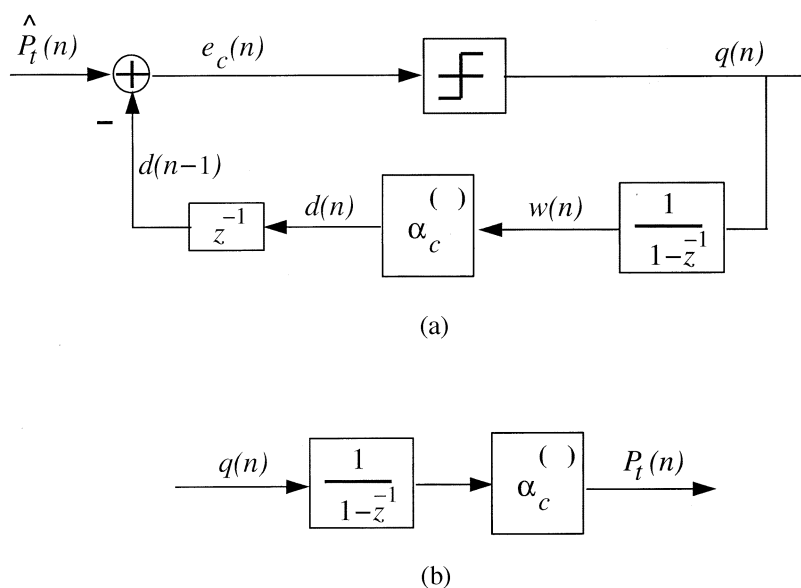

(a)

(b)

Fig. 15. Coding scheme used in the DI-CLPC algorithm. (a) Encoder and (b) decoder.

This information is to be transmitted to the MS. Since we are limited by the power bit rate, $\widehat{P}_t(n)$ should be coded to meet this rate.

The coding scheme used to transmit $\widehat{P}_t(n)$ could be the adaptation part of the ADM described in [15], [16]. This coder exhibits strong tracking, good stability, and high dynamic range. Fig. 15 shows a block diagram of the coding scheme; the encoder and decoder are shown in parts a and b, respectively. The equations describing the dynamics of the coder are

$$e_c(n) = \widehat{P}_t(n) - d(n-1), \quad d(0) = d_0$$
$$q(n) = \mathrm{sign}[e_c(n)]$$
$$w(n) = w(n-1) + q(n), \quad w(0) = 0$$
$$d(n) = \alpha_c^{w(n)}.$$

In this algorithm, the term α_c denotes the coding exponent (the subscript c is added to distinguish it from the α used in the previous algorithms). The DI-CLPC algorithm is summarized in Table III.

TABLE III
SUMMARY OF THE DIRECT INVERSE CLPC (DI-CLPC) ALGORITHM

Initialization:
Choose the desired received power P_d.
Choose the coding parameters α_c and $d(0)$.
Choose the prediction parameters:
  Filter order, μ, and U.

For every CLPC time sample $n > 0$ do:

BS.
1. Measure $P_r(n)$ from the received sequence.
2. Knowing $P_t(n-1)$, estimate $\phi(n)$.
3. Evaluate $\phi_p(n+1|n)$.
4. Code the power data $\widehat{P}_t(n) = \frac{P_d}{\phi_p(n+1|n)}$.
5. Send the coded data $q(n)$ to the MS.

MS
6. Extract $q(n)$ from the received data.
7. Use $q(n)$ to decode the power data $d(n)$.
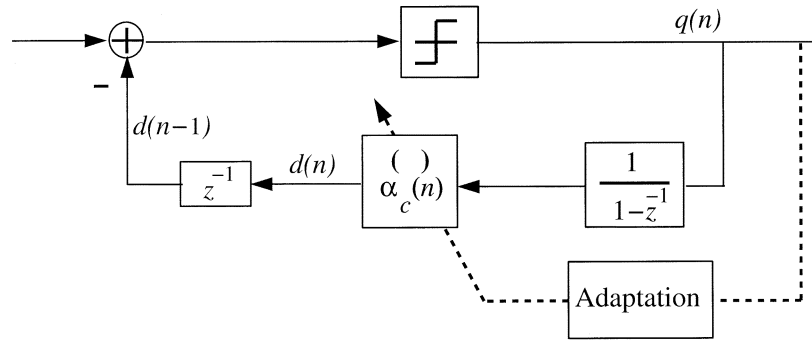8. Set $P_t(n) = d(n)$.

Fig. 16.   Coding scheme used in the ADI-CLPC Algorithm.

TABLE IV
SUMMARY OF THE ADAPTIVE DIRECT INVERSE
CLPC (ADI-CLPC) ALGORITHM

Initialization:
Choose the desired received power P_d.
Choose the prediction parameters:
  Filter order, μ, and U.
Choose the adaptation parameters:
  C, α_{max} and α_{min}.

For every CLPC time sample $n > 0$ do:

BS

1.   Measure $P_r(n)$ from the received sequence.
2.   Knowing $P_t(n-1)$, estimate $\phi(n)$.
3.   Evaluate $\phi_p(n+1|n)$
4.   Compute $\lambda(n)$ and $\alpha_c(n)$: (50) & (51).
5.   Use $\alpha_c(n)$ to code $\widehat{P}_t(n) = \frac{P_d}{\phi_p(n+1|n)}$
6.   Send the coded data $q(n)$ to the MS.

MS

7.   Extract $q(n)$ from the received data.
8.   Use (50) and (51) to recompute $\alpha_c(n)$.
9.   Decode $d(n)$ from $q(n)$ & $\alpha_c(n)$.
10. Set $P_t(n) = d(n)$.

D. Algorithm 4: Adaptive Direct Inverse CLPC (ADI-CLPC)

In the previous algorithm, the coding constant α_c has a fixed value. However, in order to provide the coder with more freedom to track high variations in the coded transmission power, the coding constant α_c can be allowed to vary, as shown in Fig. 16. The purpose of adapting α_c is similar to that in the APR-CLPC algorithm; namely, to cope with large variations in the channel power fading. Moreover, the same adaptation technique for α used in APR-CLPC is adopted here, i.e.,

$$\alpha_c(n) = \alpha_c(n-1) + \lambda(n)C \tag{50}$$

where

$$\lambda(n) = \begin{cases} +1, & \text{if } q(n) = q(n-1) = q(n-2) \\ -1, & \text{if } q(n) \neq (n-1) \\ 0, & \text{otherwise} \end{cases} \tag{51}$$

and

$$\alpha(n) = \begin{cases} \alpha_{max}, & \text{if } \alpha(n) > \alpha_{max} \\ \alpha_{min}, & \text{if } \alpha(n) < \alpha_{min} \end{cases} \tag{52}$$

with typical values $C = 0.2$, $\alpha_{max} = 2.5$ and $\alpha_{min} = 1.1$. The ADI-CLPC algorithm is summarized in Table IV.

TABLE V
POWER-CONTROL ERROR STD OBTAINED USING CONVENTIONAL CLPC

f_D (Hz)	Vehicle Speed (km/h)	PCE STD (dB)
10	6.7	0.5
20	13.36	0.7
50	33.3	1.0
85	56.7	1.2
100	66.7	1.5
150	100	2.2

V. SIMULATIONS

The algorithms developed in this article have been simulated using Matlab and Simulink. The following are the simulation parameters used:

- Desired power level P_d: 0 dB;
- Power bit rate: 1500 Hz;
- Up-sampling factor (U): 2;
- Channel type: frequency-selective multipath Rayleigh fading with two taps and variable mobile speed.

The channel-fading data was obtained using Simulink. The standard deviation of the PCE is used as a measure of how well the power-control algorithms achieve the desired received power. The exponent term α and the prediction step size μ are chosen as 1.3 and 0.8, respectively, unless otherwise specified. The standard deviations of the PCE obtained from conventional CLPC for different Doppler frequencies are shown in Table V for reference.

We start our tests by investigating the effect of μ and α on the performance of the PR-CLPC algorithm. Fig. 17 shows the effect of choosing different μ on the PCE standard deviation for different values of f_D. Choosing $\mu = 0.85$ results in best performance as indicated by the vertical heavy arrow in the figure. This PCE can be further reduced depending on the choice of the exponent term α, as shown in Fig. 18. The optimal PCE changes in a nonlinear fashion with respect to α. When the Doppler frequency of the mobile unit can be measured, then we can refer to Fig. 18 for the optimal choice of α. However, if the Doppler frequency cannot be measured accurately, then a choice of $\alpha = 1.3$ seems to be reasonable, as indicated by the vertical arrow in the figure.

The APR-CLPC algorithm is tested via simulations. Fig. 19 shows the STD of the PCE for two different values of the adaptation constant C. The saturation limits for α are chosen as
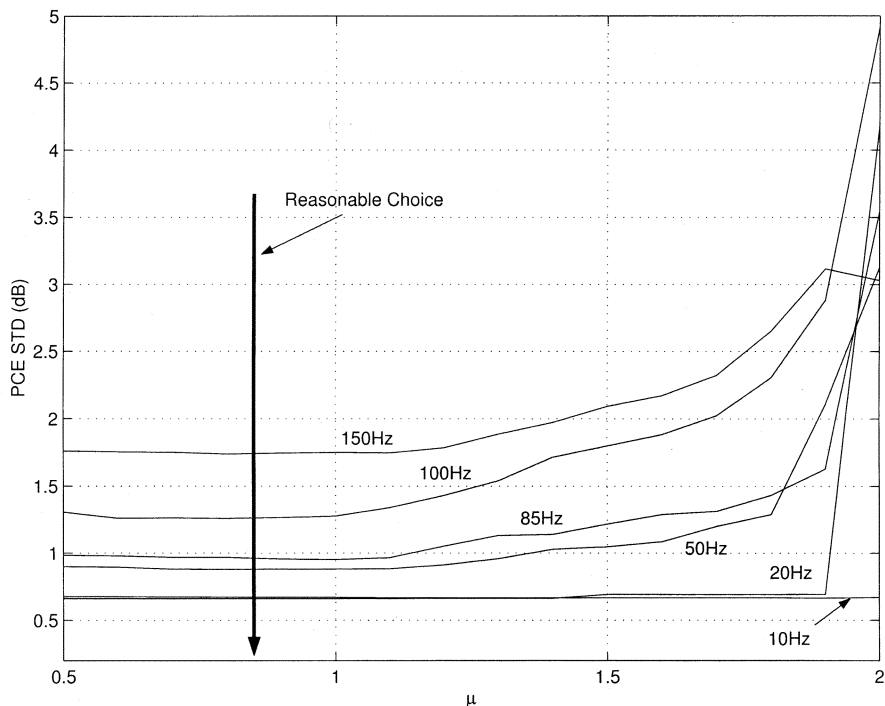
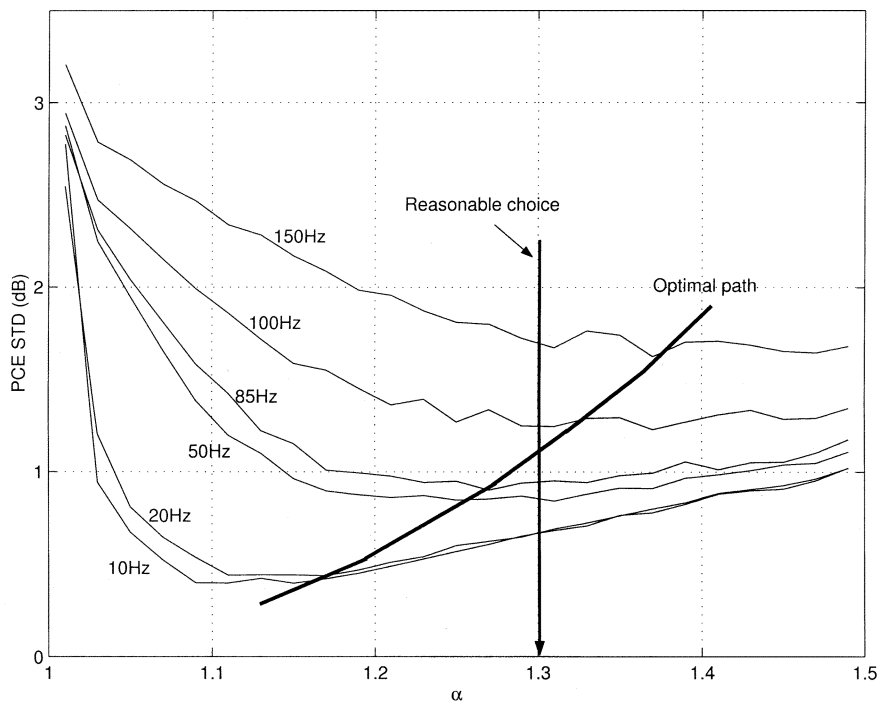Fig. 17. Effect of choosing μ on PCE for the PR-CLPC algorithm using $\alpha = 1.3$.

Fig. 18. Effect of choosing α on PCE for the PR-CLPC algorithm.

$\alpha_{\min} = 1.1$ and $\alpha_{\max} = 2$. Increasing C will improve the performance of the CLPC algorithm at high vehicle speeds, but will degrade it at low speeds. Choosing $C = 0.1$ was found reasonable for all tested applications.

Fig. 20 shows a typical response of the adaptive coding term $\alpha_c(n)$, used in the ADI-CLPC algorithm as a function of time with $f_D = 85$ Hz. The mean and variance values for $\alpha_c(n)$ in this example are 1.22 and 0.02, respectively.
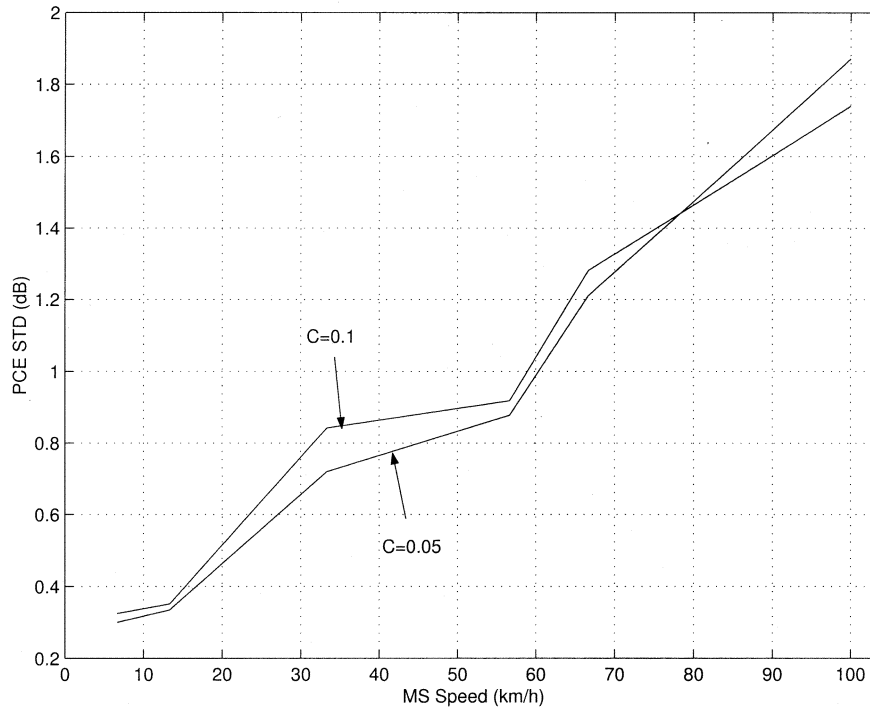
Fig. 19. Power errors for the APR-CLPC algorithm for two values of the adaptation constant C.
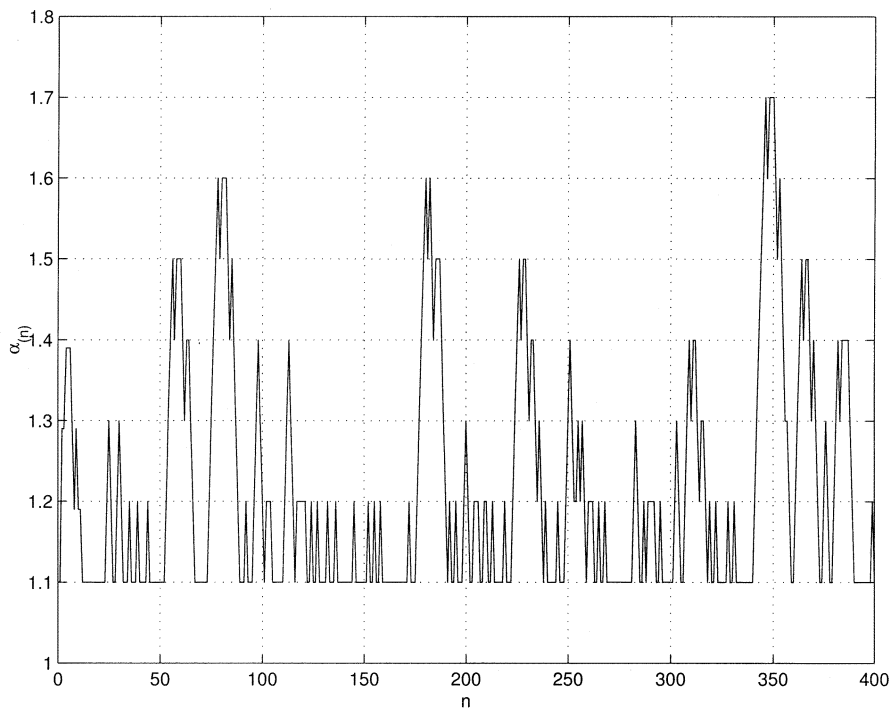

Fig. 20. A typical response for the exponent term $\alpha_c(n)$ of the ADI-CLPC algorithm over time for a Rayleigh-fading channel with $f_D = 85$ Hz.

Finally, Fig. 21 shows the PCE performance of the PR-CLPC, APR-CLPC, DI-CLPC, and ADI-CLPC. The coding parameters $d(0)$ and α_c used in the DI-CLPC algorithm are chosen as 1E-3 and 1.8, respectively. Moreover, the parameters C, $\alpha_{\min}$, $\alpha_{\max}$ for the ADI-CLPC algorithm are set to 0.1, 1.1, and 2, respectively. Fig. 21 also includes the performance of the conventional CLPC and that of an adaptive CLPC developed in [17], for the sake of comparison. The ADI-CLPC demonstrates the best performance over all other algorithms. Although the power period is an important parameter that can affect the performance of the algorithms, only a single value is tested in this work.
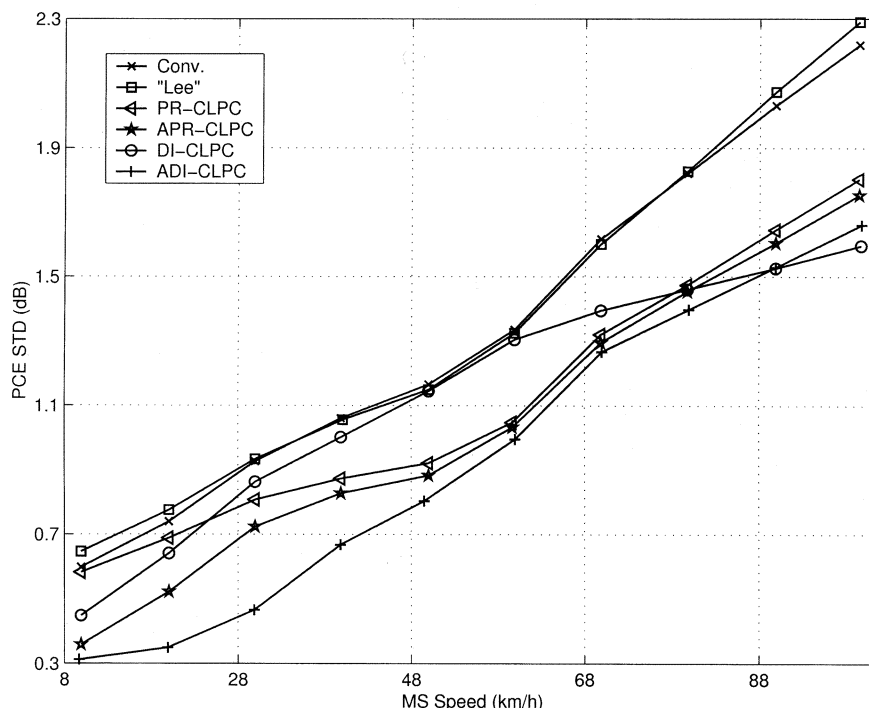
Fig. 21. Performance of the developed algorithms compared to conventional CLPC and an adaptive CLPC developed in [15].

VI. CONCLUSION

In this paper, we first explained that conventional CLPC is essentially a companded delta modulator. We then derived an expression for the PCE in conventional CLPC systems. The power error was shown to have zero mean and an expression for the error variance was derived. Several power-control schemes were proposed, which attempt to minimize the power-error variance. A prediction scheme that is based on oversampling the power measurements was used. In simulations, all proposed power-control schemes showed improved performance over the conventional scheme in terms of minimizing the power-error variance.

REFERENCES

[1] T. Ojanpera and R. Prasad, *Wideband CDMA for Third Generation Mobile Communications*. London, U.K.: Artech House, 1998.
[2] S. Nourizadeh, P. Taaghol, and R. Tafazolli, "A novel closed loop power control for UMTS," in *Proc. First Int. Conf. 3G Mobile Communication Technologies*, London, U.K., Mar, 2000, pp. 56–59.
[3] W. Xinyu, G. Ling, and L. Guoping, "Adaptive power control on the reverse link for CDMA cellular system," in *Proc. Fifth Asia Pacific Conf. Communications/Fourth Optoelectronics and Communications Conf,*, vol. 1, Beijing, China, Oct. 1999, pp. 608–611.
[4] S. Park and H. Nam, "DS/CDMA closed-loop power control with adaptive algorithm," *Electron. Lett.*, vol. 35, no. 17, pp. 1425–1427, Aug. 1999.
[5] M. Sim, E. Gunawan, B. Soong, and C. Soh, "Performance study of close-loop power control algorithms for a cellular CDMA system," *IEEE Trans. Veh. Technol.*, vol. 48, pp. 911–921, May 1999.
[6] H. Su and E. Geraniotis, "Adaptive closed-loop power control with quantized feedback and loop filtering," in *Proc. IEEE Int. Symp. Personal, Indoor and Mobile Radio Communications*, vol. 2, Boston, MA, Sept. 1998, pp. 926–931.
[7] S. Choe, T. Chulajata, H. Kwon, K. Byung-Jin, and S. Hong, "Linear prediction at base station for closed loop power control," in *Proc. IEEE Vehicular Technology Conf.*, vol. 2, Houston, TX, May 1999, pp. 1469–1473.
[8] J. Tanskanen, A. Huang, and I. Hartimo, "Predictive power estimators in CDMA closed loop power control," in *Proc. IEEE Vehicular Technology Conf.*, vol. 2, Ottawa, ON, Canada, May 1998, pp. 1091–1095.
[9] F. Lau and W. Tam, "Intelligent closed-loop power control algorithm in CDMA mobile radio system," *Electron. Lett.*, vol. 35, no. 10, pp. 785–786, May 1999.
[10] A. Abrardo and D. Sennati, "On the analytical evaluation of closed-loop power-control error statistics in DS-CDMA cellular systems," *IEEE Trans. Veh. Technol.*, vol. 49, pp. 2071–80, Nov. 2000.
[11] S. Ariyavisitaluk and L. F. Chang, "Signal and interference statistics of a CDMA system with feedback power control," *IEEE Trans. Commun.*, vol. 41, pp. 1626–1634, Nov. 1993.
[12] M. Aldajani and A. H. Sayed, "A stable structure for delta modulation with improved performance," in *Proc. Int. Conf. Acoustics, Speech, and Signal Processing*, vol. 4, Salt Lake City, UT, May 2001, pp. 2621–2624.
[13] V. Garg and J. Wilkes, *Principles and Applications of GSM*. Englewood Cliffs, NJ: Prentice-Hall, 1999.
[14] A. H. Sayed, *Fundamentals of Adaptive Filtering*. New York: Wiley, 2003.
[15] M. Aldajani and A. H. Sayed, "An adaptive structure for sigma delta modulation with improved dynamic range," in *Proc. 43rd Midwest Symp. Circuits and Systems*, vol. 1, Lansing, MI, Aug. 2000, pp. 390–394.
[16] ——, "Stability and performance analysis of an adaptive sigma delta modulator," *IEEE Trans. Circuits Syst. II*, vol. 48, pp. 233–244, Mar. 2001.
[17] C. Lee and C. Steele, "Closed-loop power control in CDMA systems," *Proc. Inst. Elect. Eng. Proc.—Commun.*, vol. 143, no. 4, pp. 231–239, Aug. 1996.

Mansour A. Aldajani (S'96–M'01) received the B.S. and M.S. degrees with first honors in systems engineering from King Fahd University of Petroleum and Minerals, Dhahran, Saudi Arabia, in 1994 and 1996, respectively. He received the Ph.D. degree in electrical engineering from the University of California, Los Angeles, in 2001.

He is an Assistant Professor of systems engineering at King Fahd University of Petroleum and Minerals. His research interests include signal processing (source coding, high-resolution sigma–delta data conversion, and adaptive filtering), digital control, and power control in wireless communication.

Dr. Aldajani is the recipient of the Prince Mohammed Ben Fahd Award for research projects in 1994, the Academic Support Activities award in 1995, and the Department Graduate Student Award in 1996.

Ali H. Sayed (S'90–M'92–SM'99–F'01) received the Ph.D. degree in electrical engineering in 1992 from Stanford University, Stanford, CA.

He is Professor and Vice Chairman of Electrical Engineering at the University of California, Los Angeles (UCLA). He is also the Principal Investigator of the UCLA Adaptive Systems Laboratory. He is the author of the textbook *Fundamentals of Adaptive Filtering* (New York: Wiley, 2003) and is the coauthor of the research monograph *Indefinite Quadratic Estimation and Control* (Philadelphia, PA: SIAM, 1999) and of the textbook *Linear Estimation* (Englewood Cliffs, NJ: Prentice-Hall, 2000). He is also coeditor of the volume *Fast Reliable Algorithms for Matrices with Structure* (Philadelphia, PA: SIAM, 1999). His research interests span several areas, including adaptive and statistical signal processing, filtering and estimation theories, signal processing for communications, interplays between signal processing and control methodologies, system theory, and fast algorithms for large-scale problems.

Dr. Sayed is a member of the editorial boards of the Society of Industrial and Applied Mathmatics *Journal on Matrix Analysis and Its Applications*, EURASIP *Journal on Signal Processing*, and the *International Journal of Adaptive Control and Signal Processing*. He has served as coeditor of special issues of the journal *Linear Algebra and Its Applications*, has contributed several articles to engineering and mathematical encyclopedias and handbooks, and has served on the program committees of several international meetings. He has also consulted with industry in the areas of adaptive filtering, adaptive equalization, and echo cancellation. His work has been awarded several recognitions, including a 1996 IEEE Donald G. Fink Award, a 2002 Best Paper Award from the IEEE Signal Processing Society, and two Best Student Paper Awards at international meetings. He serves as Editor-in-Chief of the IEEE TRANSACTIONS ON SIGNAL PROCESSING.